Draft version 0.1

# ATLAS NOTE

ATL-PHYS-PUB-2009-XXX

April 2, 2009

## Calibration of charge sharing algorithm for the ATLAS Pixel Detector using cosmic data

### Abstract

During fall 2008 ATLAS Pixel detector was commissioned registering data from cosmic rays triggered during ATLAS or Inner Detector combined runs. Using these informations the charge sharing algorithm was for the first time calibrated for the ATLAS Pixel Detector using real data.

When a charged particle crosses the Pixel Detector, the adjacent pixels that are fired are combined into a cluster. A rough estimate of the point where the particle crossed the detector can be given by the mid point of the cluster. The charge sharing algorithm use the measurement of the charge released inside the outermost pixel of the cluster to give a more precise estimate of the position crossed by the particle on the detector.

# 1 Introduction

ATLAS physics studies impose tight requirements on momentum and vertex resolution. These high-precision measurements are made in the inner detector tracking system that is composed of two silicon detectors, the Pixel detector and the silicon microstrip tracker (SCT), and of a transition radiation tracker (TRT) made by straw tubes. The whole inner detector is immersed in a 2 T magnetic field generated by the central solenoid, that permits to estimate the momentum of the particles measuring the curvature of their trajectory. The highest granularity measurement is achieved around the vertex region using silicon pixel sensors.

The pixel detector covers the region $|\eta| < 2.5$. It has approximately 80.4 million readout channels and it is composed of identical modules containing each 46.080 pixels. The tipical pixel size is $50 \times 400$ $\mu$m$^2$. In the barrel region modules are arranged on concentric cylinders around the beam axis while in the end-cap regions, they are located on disks perpendicular to the beam axis. The pixel layers are segmented in $R - \phi$ and $z$ with typically three pixel layers crossed by each track. The first layer, called the "b-layer", is at a radius of 51 mm. The intrinsic resolution for the pixel detector measurements are showed in Table 1 while a full description of this detector can be found in [1].

Each part of the inner detector should be aligned with the best possible precision. Cosmic rays data gave the possibility to estimate and correct the alignment of the pixel detector components to a precision of about 20 $\mu$m. **(This should be referenced, the value is the one that will be used for mc09 simulation)** . This level of alignment is comparable with the tolerance for the axial direction, but is still preliminary respect to the radial and azimuthal expectation (see Table 1). The effect of misalignment should be taken into account when the impact of charge sharing calibration on the resolution is evaluated.

| Pixel structure | Intrinsic accuracy ($\mu$m) | | Alignment tolerances ($\mu$m) | | |
|---|---|---|---|---|---|
| | Azimuth (R-$\phi$) | Axial (z) | Radial (R) | Axial (z) | Azimuth (R-$\phi$) |
| b-layer | 10 | 115 | 10 | 20 | 7 |
| Layer 1 & 2 | 10 | 115 | 20 | 20 | 7 |
| Disks | 10 | 115 | 20 | 100 | 7 |

Table 1: Intrinsic measurement accuracies and mechanical alignment tolerances for the pixel sub-structures, as defined by the performance requirements of the ATLAS experiment. Tolerances correspond to the single-module accuracy. Values are taken from [2].

## 1.1 Digital position

The pixel detector should measure the position of particles coming from interactions with a precision Just the explanation of the digital alghoritm...

Should contain the explanation of $\eta$ and $\phi$ direction.

Also ask to Attilio (that already told me...) the difference between "analog with 0 constants" and "pure digital".

## 1.2 Analog position

Here the formula for the digital position

$$x_{\text{analog}} = x_{\text{digital}} + \Delta \times \left( \frac{q_1}{q_1 + q_2} - \frac{1}{2} \right) \tag{1}$$

should be explained. Also I want to report some residual (G4 hit - analog/digital position) distribution (for both direction) that shows at G4 hit level which is the improvement that can be expected from the "analog" procedure. **Lidia should look into this whith her MC tool.**

It should be explained that the $\frac{q_1}{q_1+q_2}$ factor is measured by pixels informations themselves, knowing the charge released in the first ($q_1$) and in the last ($q_2$) pixel of the cluster. As opposite, the $\Delta$ should be measure from reconstructed data. In general we expect that it is depending on incidence angle, that is computed only when the "track" associated to the particle is reconstructed.

All procedure can be described only for cluster size 2 and then add a note saying that it is valid (but less efficient) also for bigger cluster size.

# 2 Extraction of constants from cosmic data

General description of the procedure: fit of the distribution *Digital residual vs* $\frac{q_1}{q_1+q_2}$ (see figure 1).

Brief discussion on why this distribution sholud allow the extraction of $\Delta$ and of the fact thet we expect the distribution to shift but not to change the angular coefficient when we change the alignment of the detector.

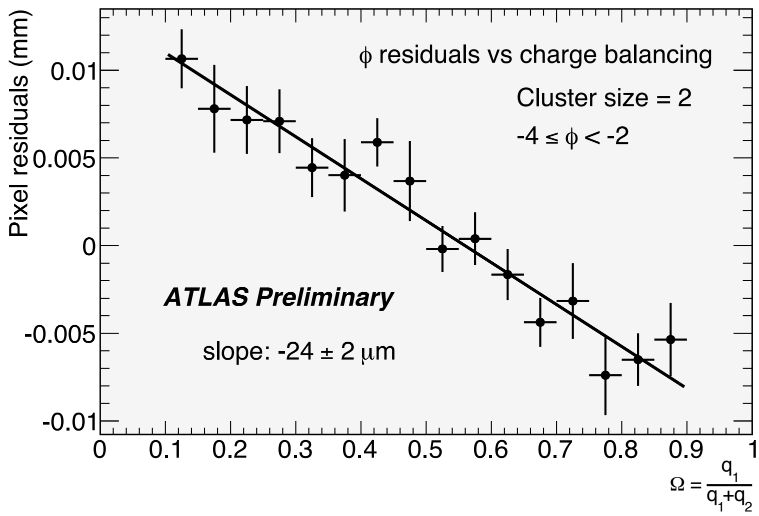


Figure 1: Example of a fit

## 2.1 Description of data used and cut applied

Only "field on" data, first and second reprocessing (that means better alignment!). Distribution of tracks in $\eta$ and $\phi$, relative abundance of cluster size 1, 2 and 3 clusters at each angle (to be added, no difference in the two sets of data).

The cuts that were applied are the following:

- reflection of the angle if track is going upward
- cut on residuals accordig to momentum: rescut = sqrt( (0.5/GeVTrkPt)*(0.5/GeVTrkPt) + HighPtRes*HighPtRes); (maybe a plot should justify this. . . )

### 2.2 Result of the fit

Constants were extracted for each layer at different incidence angles. Different cluster sizes were fitted separately (Figure 2, should be updated, different colors for the two sets. . . ). Constants are fitted for first processing and reprocessing and the values are the same.

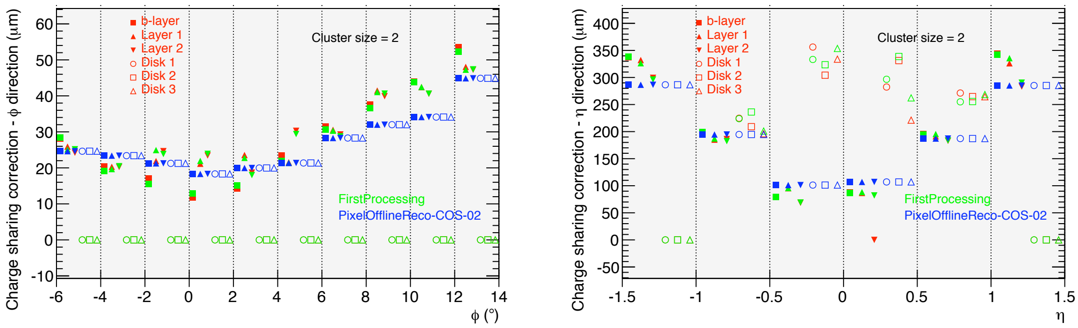


(a) Constants for $\phi$ direction

(b) Constants for $\eta$ direction

Figure 2: Red markers represent the constanst fitted from the reprocessing of data with final alignmenta. They are compared with the constants fitted from data reconstructed with preliminary alignment (green) and with the constants that were recorded in the database (tag PixelOfflineReco-COS-02, blue).

# 3 Validation of constants and effects on resolution

The validation of the constants has been performed following two criteria:

### 3.1 Fit of the analog residuals vs charge sharing distribution

The correction is fitted as the angular coefficient of "uncalibrated data". The same distribution for "calibrated data" is expected to be flat. Some more comments. . . a figure?

### 3.2 Residual distribution improvement

The analog position is known to be a better approssimation of the position in which the particle crossed the detector. This should reflect in an improvement of the track quality. In particular the residual distribution (extrapolated position - measured position) should be narrower for analog positions.

The whole sample of tracks was reconstructed using exaclty the same calibration constants except for the chrge sharing and umbiased residuals were used to compare the "calibrated data" with the "uncalibrated ones" (see figure 3).

First of all the effect of each single constant was checked (figure 3(c)), then the global effect for cluster size 2 clusters for both directions (figure 3(a) and 3(b)) and the global effect for each layer (to be added).

The improvement appear to be much more evident for $\eta$ direction. This should be discussed: the biggest (in absolute value) improvement for $\eta$ is surely due to the fact that pixels are bigger in this direction. The bigger impact (in percentage) on resolution for $\eta$ is maybe due to the worst alignment (respect to final expectation) for $\phi$ direction. Also MC study (and some literature i.e. [3]) should help to clarify if this point is expected or not..

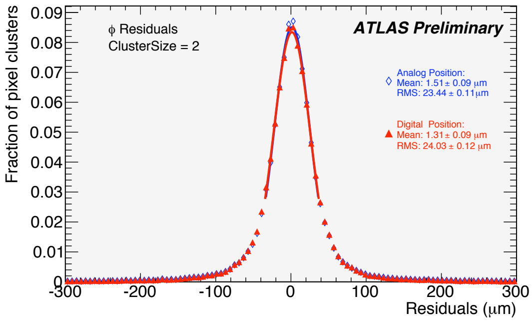


(a) $\phi$ direction, clusters made by 2 hits

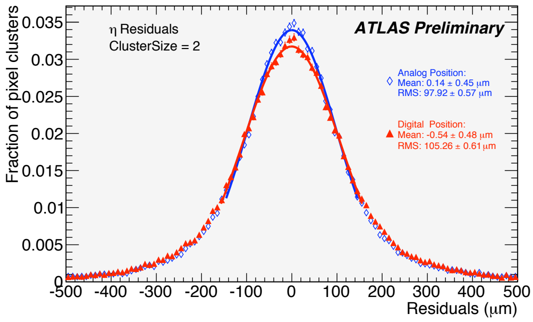


(b) $\eta$ direction, clusters made by 2 hits

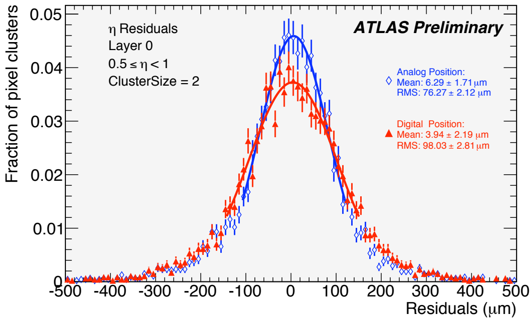


(c) $\eta$ direction, clusters made of 2 hits, fixed incidence angle ($0.5 < \eta < 1.0$)

Figure 3: Improvements in resolution

## 3.3 Resolution vs incidence angle

Resolution in the pixel detector is dependent upon incidence angle of particles (see [3]). For the analog resolution we expect to have a worsening of resolution increasing the incidence angle. For the digital algorithm we have a big improvement of resolution for cluster size 2 that brings to a minimum in the distribution of residuals vs incidence angle. The minimum is expected for the angle at which the fraction of cluster size 2 clusters is bigger (equal?) to the fraction of clustersize 1 clusters. We report here this distribution and we compare the minimum with the expected value. Of course extrapolation errors (both absolute value and dependence on track direction) are totally different for test beam and cosmics with final geometry!!

## 3.4 Validation with Montecarlo data

We can see if on some data with a “perfect” alignment we notice a bigger impact on $\phi$ resolution.

Also we can compare here the constants from test beam and the one from cosmics.

Constants extracted from montecarlo can be compared with constant extracted from data.

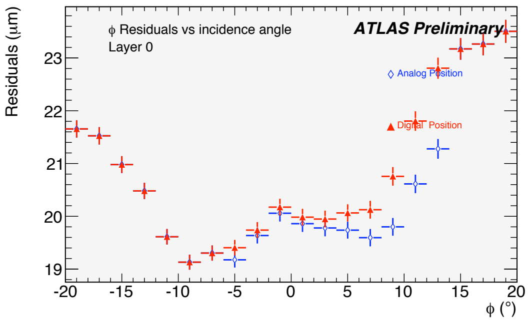


(a) $\phi$ direction

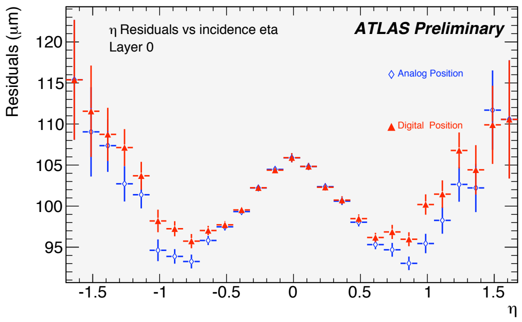


(b) $\eta$ direction

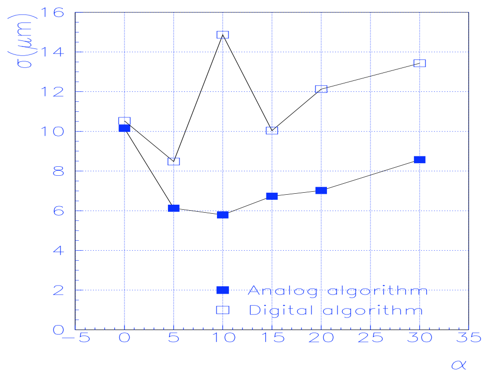


(c) Test beam

Figure 4: Resolution as a function of angle.Test beam plot from [3]. ATLAS Preliminary should be removed from figure, graphical aspect should be changed!

# 4 Comments on the values obtained for constants

These are interesting point for some discussion:

- the extraction of constants was performed over data that were reconstructed with different aligne-ment constants: the fit results were confirmed to be indipendent from alignment
- extracted constants were compared to the ones extracted during test beam: they appear to be the same for $\phi$ direction, while they are roughly half of the TB value for $\eta$ direction
- Since the constants were not extracted for disks and values for different layer were very similar, a common fit for all layer was performed and obtained constants were committed to the DataBase for future reconstruction (see figure 5).
- we expect a minima in 0 incidence angle and a pattern that is simmetrical around it. This is not fully seen for $\phi$ direction.
- constants for clustersize $> 2$ were not extracted due to poor statistics (true??) we expect them to be smaller than the one for cluster size 2.

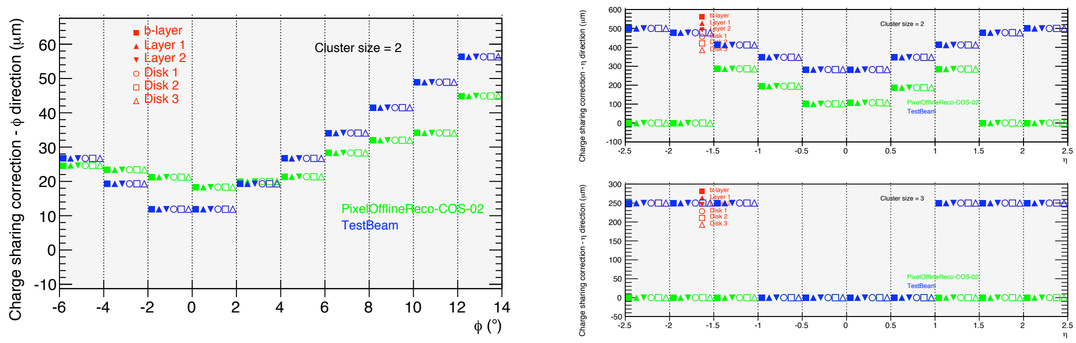


(a) Constants for $\phi$ direction (b) Constants for $\eta$ direction

Figure 5: Constants submitted to database for future use in reconstruction

# References

[1] G. Aad, M. Ackers, F. A. Alberti, M. Aleppo, G. Alimonti, J. Alonso, E. C. Anderssen, A. Andreani, A. Andreazza, J.-F. Arguin, K. E. Arms, D. Barberis, M. B. Barbero, M. Bazalova, R. B. Beccherle, K. H. Becks, P. K. Behera, F. Bellina, J. Beringer, K. Bernardet, J. B. Biesiada, L. Blanquart, J. Boek, G. R. Boyd, P. Breugnon, P. Buchholz, B. Butler, M. Caccia, A. C. Capsoni, C. Caso, D. Cauz, M. Cepeda, R. Cereseto, M. Cervetto, M. L. Chu, M. Citterio, J. C. Clemens, Y. C. Coadou, M. Cobal, A. Coccaro, S. Coelli, S. Corrard, M. Cristinziani, S. Cuneo, S. Dauria, M. Dameri, G. Darbo, S. Dardin, B. DeLotto, U. De Sanctis, J. B. De Vivie De Regie, C. del Papa, P. Delpierre, B. Di Girolamo, W. Dietsche, F. Djama, D. Dobos, M. Donega, J. Dopke, K. Einsweiler, A. Eyring, D. Fasching, L. Feligioni, D. Ferguson, W. Fernando, P. Fischer, M. J. Fisher, T. Flick, G. Gagliardi, E. Galyaev, K. K. Gan, M. Garca-Sciveres, N. Garelli, G. G. Gariano, G. G. Gaycken, C. Gemme, P. Gerlach, M. G. D. Gilchriese, M. P. Giordani, D. Giugni, K. W.

Glitza, C. Gssling, T. Golling, F. Goozen, I. Gorelov, G. Gorfine, C. Grah, H. M. Gray, I. M. Gregor, J. Grosse-Knetter, K. Grybel, P. Guterrez, G. D. Hallewell, N. Hartman, M. Havranek, B. Heinemann, T. Hen, M. R. Hoeferkamp, D. Hoffmann, M. Holder, W. Honerbach, C. Horn, S. Hou, G. S. Huang, F. Huegging, E. W. Hughes, I. Ibragimov, I. Ilyashenko, M. Imhaeuser, J. M. Izen, J. Jackson, D. Jana, R. C. Jared, P. Jez, T. Johnson, J. Joseph, H. Kagan, M. Karagounis, R. D. Kass, M. Keil, S. Kersten, P. Kind, J. Klaiber-Lodewigs, L. Klingbeil, R. Klingenberg, A. Korn, V. V. Kostyukhin, I. Kostyukhina, O. Krasel, H. Krger, K. Krger, J. Kudlaty, T. Khl, O. Kvasnicka, K. Lantzsch, T. Lari, S. L. Latorre, S. C. Lee, T. Lenz, G. Lenzen, J. Lepidis, J. Levłque, M. Leyton, D. Lopez Mateos, K. F. Loureiro, D. Lke, L. Luisa, J. Lys, R. J. Madaras, P. Mttig, F. M. Manca, E. Mandelli, M. Marcisovsky, Z. Marshall, G. Martnez, L. Masetti, M. Ma, M. Mathes, R. McKay, G. Meddeler, R. Meera-Lebbai, C. Meroni, J. Metcalfe, W. T. Meyer, D. W. Miller, W. Miller, S. Montesano, M. M. Monti, P. Morettini, J. M. Moss, T. Mouthuy, P. Nechaeva, W. Ockenfels, G. A. Odino, M. Olcese, B. Osculati, F. Parodi, A. Pekedis, K. Perez, I. Peric, C. Pizzorno, J. Popule, R. Post, F. Ragusa, A. M. Rahimi, B. Raith, S. Rajek, K. Reeves, I. Reisinger, J. D. Richardson, E. I. Rosenberg, L. P. Rossi, I. Rottlnder, A. R. Rovani, A. Rozanov, O. Runlfsson, E. R. Ruscino, A. F. Saavedra, F. S. Sabatini, M. Saleem, S. Sandvoss, B. Sanny, L. Santi, M. I. Scherzer, C. Schiavi, A. Schreiner, J. Schultes, A. Schwartzman, R. Seibert, S. C. Seidel, H. Severini, S. Shanava, P. Scho, P. Skubic, A. C. Smith, D. S. Smith, J. Snow, T. Stahl, T. Stockmanns, S. Strandberg, M. Strauss, D. Ta, F. Tegenfeldt, P. K. Teng, R. Ter-Antonian, J. Thadome, T. Tic, L. Tomasek, M. Tomasek, F. Tomasi, K. Toms, C. Tran, J. Treis, N. Triplett, C. Troncon, L. Vacavant, S. Vahsen, J. Valenta, G. Vegni, F. Vernocchi, E. Vigeolas, J. Virzi, E. Viscione, V. Vrba, J. Walbersloh, W. Walkowiak, J. Weber, T. F. Weber, J. Weingarten, C. Weldon, N. Wermes, U. Werthenbach, J. S. Wirth, R. Witharm, B. Witt, M. Wittgen, J. Wstenfeld, R. Wunstorf, J. Wyckoff, W.-M. Yao, C. Young, R. Zaidan, M. Zdrazil, F. Zetti, J. Zhong, M. Ziolkowski, G. Zizka, and M. M. Zoeller, *ATLAS pixel detector electronics and sensors*, J. Instrum. **3** (2008) P07007.

[2] The ATLAS Collaboration, *Expected Performance of the ATLAS Experiment: Detector, Trigger and Physics*. CERN, Geneva, 2008.

[3] T. Lari and F. Ragusa, *Study of silicon pixel sensors for the ATLAS detector*. PhD thesis, Milan Univ., Geneva, 2001. Presented on 12 Dec 2001.